Al-Mustansiriyah Journal of Science
ISSN: 1814-635X (print), ISSN:2521-3520 (online) Volume 32, Issue 3, 2021 DOI: http://doi.org/10.23851/mjs.v32i3.967

Research Article **Open Access**

Effects of Change PH on the Structural and Optical Properties of Iron Oxide Nanoparticles

Raad S. Sabry, Muslim A. Abid, Sarah Q. Hussein*

Department of Physics, College of Science, Mustansiriyah University, Baghdad, IRAQ.

*Correspondent email: sarahnoend@gmail.com

ArticleInfo

Received
16/04/2021

Accepted
26/05/2021

Published
20/06/2021

ABSTRACT

Iron oxide nanoparticles were made using celery extract by chemical method with change PH. Bio-materials in celery extract synthesized the iron oxide nanoparticles by reducing iron (III) chloride ($FeCl_3$) and then acted as both capping and stabilizing agents. The iron oxide NPs were characterized by XRD, SEM, and UV–vis techniques. The change PH affected the size, shape, and purity of iron oxide NPs. XRD results showed Crystallite size increased from 16.71nm to 21.65nm as pH was increased from 1.6 to 12. SEM images showed that the particle size of (α-Fe_2O_3) NPs was around 40.06 nm, while increasing PH showed different shapes in the same sample. The particle size became approximately 45.56 and 61.22 nm. UV–vis measurements showed the energy band increased from 3.11eV to 5.11eV. The antimicrobial activity of iron oxide NPs was determined by growth inhibition zones of the negative gram bacteria *E. coli*, *Klebsiella spp*, and gram-positive bacteria *S. aureus*, *S. epidermidis*, and fungal *Candida albicans*. The zones for (α-Fe_2O_3) NPs when PH 1.6 was between (12-13) mm. The zones for (α-Fe_2O_3) NPs when PH 12 was a little higher between (13-15) mm.

KEYWORDS: Iron Oxide nanoparticles; Bio-materials; Structural and optical properties.

الخلاصة

تم تصنيع جزيئات أكسيد الحديد النانوية باستخدام مستخلص الكرفس بالطريقة الكيميائية مع تغييرالرقم الهيدروجيني. صنعت المواد الحيوية في مستخلص الكرفس جزيئات أكسيد الحديد النانوية عن طريق تقليل كلوريد الحديد الثلاثية ($FeCl_3$) ثم عملت كعوامل للتثبيت والاستقرار. تم تمييز جسيمات أوكسيد الحديد النانويه بتقنيات حيود الأشعة السينية والمجهر الالكتروني الماسح ومطياف الاشعه فوق البنفسجيه. أثر تغيير الرقم الهيدروجيني على حجم وشكل ونقاء جسيمات أوكسيد الحديد النانويه. أظهر حيود الأشعة السينية زيادة حجم البلورات من 16.71 نانومتر إلى 21.65 نانومتر مع زيادة الرقم الهيدروجيني من 1.6 إلى 12. أظهرت صور المجهر الإلكتروني الماسح أن حجم الجسيمات النانوية(α-Fe_2O_3) كان حوالي 40.06 نانومتر ، بينما عند زيادة الرقم الهيدروجيني تظهر أشكالًا مختلفة في نفس عينة. أصبح حجم الجسيمات حوالي 45.56 و 61.22 نانومتر. أظهرت قياسات مطياف الاشعة فوق البنفسجية زيادة نطاق الطاقة 3.11 eV الى 5.11 eV . تم تحديد النشاط المضاد للميكروبات لأوكسيد الحديد من خلال أقطار تثبيط نمو بكتريا سالبة الغرام (الإشريكية القولونية، الكلبسيلة الرئوية) وبكتريا موجبة الغرام (العصوية الرقيقة، مكورة عنقودية ذهبية(و ضد فطر (فطر المبيض) .الأقطار للجسيمات النانوية(α-Fe_2O_3) عندما كان الرقم الهيدروجيني 1.6 بين (12-13) ملم. الأقطار للجسيمات النانوية(α-Fe_2O_3) عندما كان الرقم الهيدروجيني 12 أعلى قليلاً بين (13-15) ملم

INTRODUCTION

In recent years, nanotechnology has become a common and essential technology. Nanotechnology itself addresses nanoparticles that are atomic or molecular aggregates with a scale of fewer than 100 nanometers [1]. Metal oxide NPs are usually considered to be healthy for humans and the environment among the various NPs [2]. The most common metal oxides are titanium dioxide (TiO_2), copper oxide (CuO), zinc oxide (ZnO), bismuth oxide (Bi_2O_3), and iron oxide (Fe_2O_3) [3]. Because of their small size, high magnetism, and low toxicity, iron oxide nanoparticles are widely used [4]. Iron oxide comes in several forms. One of the three primary forms of iron oxides is iron (III) oxide, also known as ferric oxide. It is reddish-brown, semi-magnetic, and often called rust [5]. Drug delivery, wastewater treatment, cancer therapy, and magnetic resonance imaging (MRI) all benefit from iron oxide nanoparticles [6]. Green synthesis is superior to physical and chemical methods for reducing environmental risk because it is an easy, cost-effective, and environmentally friendly process. This approach does not necessitate the use of high pressure, high temperature, large

amounts of energy, or harmful chemicals [7]. Plant and bacterial-mediated methods have developed new synthetic techniques for creating a variety of green chemistry to synthesize nanomaterial [8]. In this study, Iron oxide nanoparticles were made using celery extract by chemical method with change PH. The iron oxide forms were determined using X-ray diffraction (XRD) analysis. The scale, morphology, and distribution of iron oxide nanoparticles were studied using scanning electron microscopy (SEM). The absorption spectrum of iron oxide nanoparticles was obtained using UV-visible spectroscopy. Finally, the antibacterial activity was investigated by the well diffusion method.

EXPERIMENTAL PROCEDURE

Materials and methods

Iron salt ($FeCl_3$) and the plant sample were purchased from the local market in Baghdad, negative Gram bacteria (*Escherichia coli*, *Klebsiella spp*) positive Gram e bacteria (*Staphylococcus*, *S. epidermidis*), and *Candida albicans* were obtained from the Department of biology, College of Science, Mustansiriyah University.

Preparation of Celery extract

The Celery leaves were washed with distilled water for the removal of dust and dirt. Around 10 g of leaves were chopped and boiled for 120 minutes at 80 °C in 100 ml deionized water. Then filtered the extract in burette to use as a reducing and capping agent.

Preparation of IONPs from Celery extract

Iron oxide NPs were created by adding 125 ml of Celery extract to (0.25 M, 4.05 gm, 100 ml) of FeCl3 Dropwise slowly. Then, mix the reaction materials and pass about 40 minutes. Color change indicates the formation of iron oxide nanoparticles. Finally, for 2 hours at 200oC, the solution is put in the ceramic eyelid in the oven and left in the oven to obtain the nano-iron oxide powder. Eq. (1) provides the chemical reaction to obtain (α-Fe_2O_3) NPs [9].

$$FeCl_3 + H_2O = Fe^{3+} \xrightarrow{Celery\ Extract} o = Fe - o - Fe = o \qquad (1)$$

The pH was changed from 1.6 to 12 by adding NaOH (14M) and examined with a pH scale on a magnetic stirrer to show the effect of the pH on the iron oxide nanoparticles.

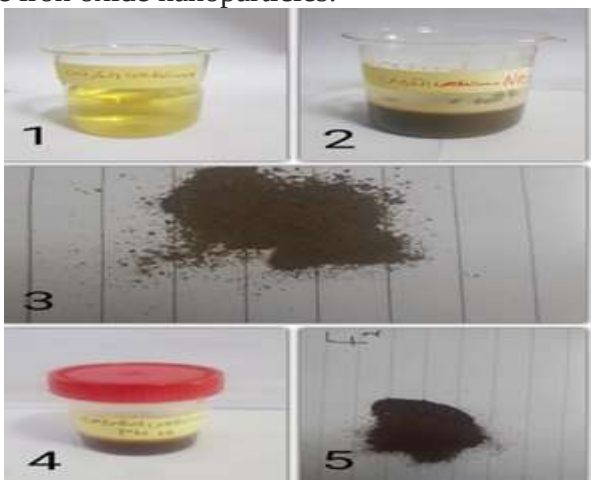

Figure 1: Synthesis of α-Fe_2O_3 nanoparticles, 1. Celery extract, 2. IONPs when PH (1.6), 3. Powder when PH (1.6), 4. IONPs when PH (12), 5. Powder when PH (12).

Characterization of IONPs

The obtained samples were confirmed using a step scan mode (XRD-6000, Shimadzu) in the 2θ angles ranging from 30° to 80°. The morphologies, microscopic structural, and size distribution of as-synthesized iron oxide Nps samples were characterized by using a scanning electron microscope Tescan Mira3 SEM, Czech Republic) in Iran. The UV–vis spectrum of the colloidal solution was determined with a spectrophotometer (UV-1800, Shimadzu).

Antimicrobial activity of IONPs

The antimicrobial property of synthesized α-Fe_2O_3-NPs was tested to investigate the herbal functionality of NPs. Antimicrobial activity was determined via the agar well diffusion method [10]. For the antimicrobial test, the organisms used were negative Gram bacteria (*Escherichia coli*, *Klebsiella spp*), Positive Gram bacteria are (*Staphylococcus*, *S. epidermidis*) and *Candida albicans*. The percentages of inhibition zones were calculated using the equation below [11].

$$Inhibition\ Zone\ (\%) = \frac{Diameter\ of\ the\ inhibition\ zone\ in\ mm}{Diameter\ of\ pertiplate(90mm)} * 100\% \qquad (2)$$

RESULTS AND DISCUSSION

Structural Properties

X-ray diffraction

The crystal planes of (104), (110), (202), (116), and (125) specify the formation of Hematite (α-Fe_2O_3) nanoparticles in both cases, according to

the XRD patterns shown in Fig. (2). This result agrees with [12]. All of the reflection peaks are in good agreement with the rhombohedral structure of (α-Fe_2O_3) as predicted. The average crystallite sizes were found to be around 16.71nm when PH 1.6 and 21.65 nm when PH 12. When pH increases to 12 the impurities are eliminated and the material becomes more pure. This may be due to the fact that FeCl3 is not reduced completely to nano Fe, when the pH is raised; all $FeCl_3$ has been reduced to nano Fe. The peak intensities of Fe NPs are increasing when (pH 12) and become more regular compared with PH 1.6.

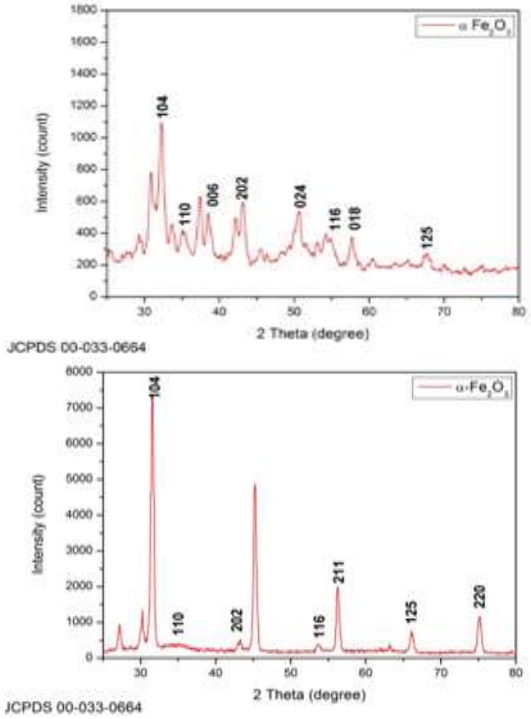

Figure 2. XRD data of α-Fe_2O_3 nanoparticles.

Morphological properties

The morphology and particle size were studied using the SEM. when PH 1.6. a micrograph of the nanoparticle structures observed with the particle size of 40.06 nm is shown in Figure (3-a). Figure (3-b) (A) Presents FE-SEM of synthesized (α-Fe_2O_3) NPs when PH 12. A micrograph reveals that the shape of the particles was influenced by the experimental conditions and shows different shapes in the same sample. The NPs aggregation of small NPs to Sheet shape and cubic with particle size 61.22 and 45.56 nm respectively.

Optical properties

UV-Vis absorption spectrum

Figure 4 shows the energy band gap of (α-Fe_2O_3) NPs, determined by drawing the square $(\alpha h\upsilon)^2$ against the energy of the photon ($h\upsilon$). The energy band gap is calculated by extrapolating the straight line to $(\alpha h\upsilon)^2$. The value of the optical band gap of (α-Fe_2O_3) NPs is 3.11eV. An increase in the pH value was observed as an increase in the absorbance at 223 nm up to a pH 12[9]. Therefore, the increase in pH increases the energy gap, the value of the bandgap of (α-Fe_2O_3) NPs at PH 12 is 5.51eV.

Antibacterial activity

The antimicrobial activity of iron oxide NPs synthesized was investigated against Gram-positive (*S. aureus*, *S. epidermidis*) and Gram-negative (*Escherichia coli*, *Klebsiella spp*) bacterial cultures, as well as fungal cultures (*Candida albicans*). The ability of the antibacterial agent NPs to rupture bacterial cells was tested using the good diffusion method. Iron oxide NPs were dissolved in Dimethyl Sulphoxide (DMSO) solvent with a concentration (40 mg/ml).

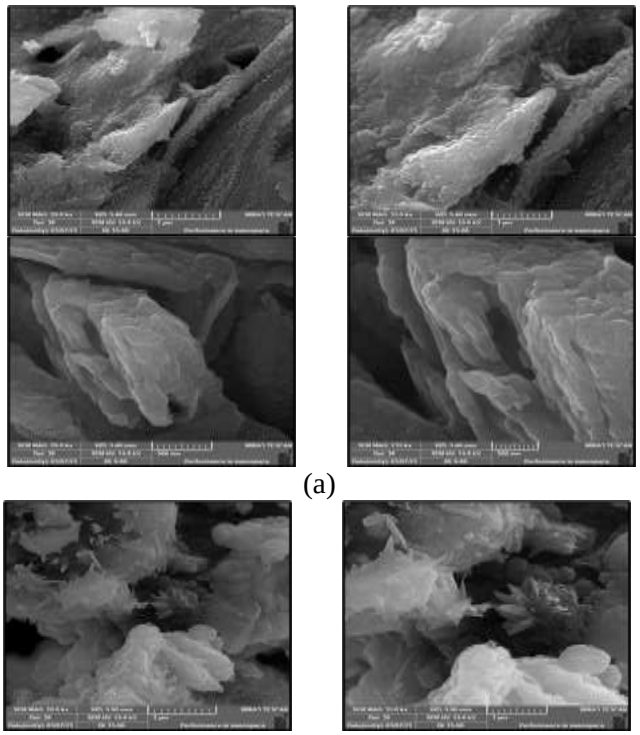

(a)

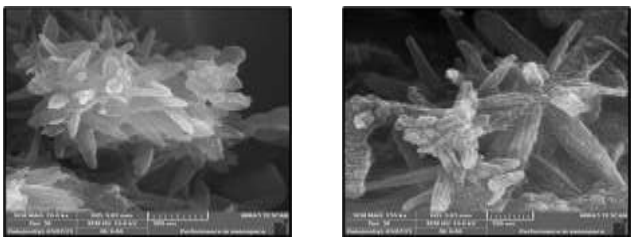

(b)

Figure 3. FESEM images of (a) when PH 1.6, (b) when PH 12.

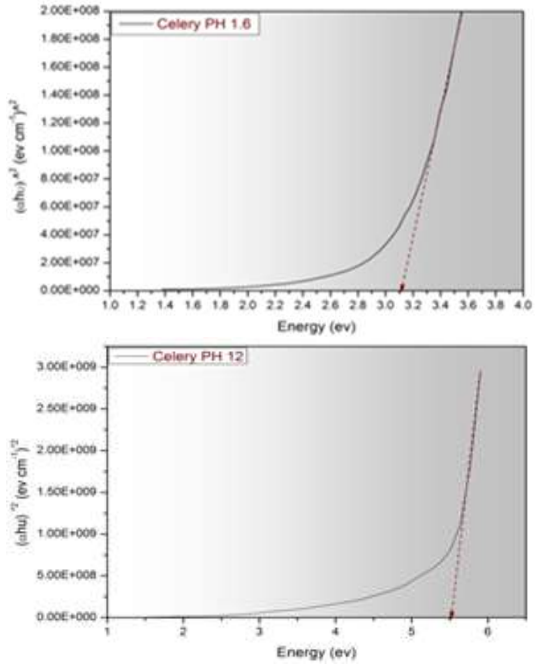

Figure 4. Energy band gap of nano α-Fe_2O_3 NPs.

The antibacterial properties of the nanoparticles are because of their nanoscale size that allows assembly or sedimentation on the surface of the bacterial strains under investigation [10]. Plant extracts, in addition to NPs, can have antibacterial activity due to the existence of phytochemical components [2]. The antibacterial activity of iron oxide NP at PH 1.6 and 12 is primarily due to the release of iron ions, which are all electrostatically attracted to the bacterial cell wall. Furthermore, metal ions are capable of penetrating within bacteria as well as communicating with the membrane's surface. The antibacterial activity of iron oxide NP at PH 1.6 and 12 is primarily due to the release of iron ions, which are all electrostatically attracted to the bacterial cell wall. Furthermore, metal ions are capable of penetrating within bacteria as well as communicating with the membrane's surface. NPs can react with the thiol group (-SH) in the bacteria's cell wall, preventing nutrients from being transported through the cell wall. The protein decreases inside the cell, ultimately leading to cellular death [11]. The IONPs obviously had antibacterial properties, and the same effect was seen with both gram-negative.

Table 1. Inhibition zone results of IONPs.

The name of the microbe	PH 1.6	PH 12
S. aureus	13 mm	13 mm
S. epidermidis	13 mm	13 mm
E. coli	13 mm	13 mm
Klebsiella spp	12 mm	13 mm
Candida albicans	13 mm	15 mm

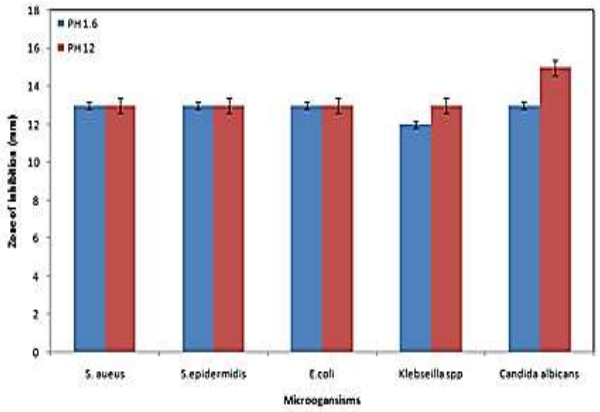

Diagram 1. Antimicrobial potency of biosynthesized.

Figure 5. Antimicrobial activity of α-Fe_2O_3.

CONCLUSIONS

Celery extracts with $FeCl_3$ were used to synthesize iron oxide NPs using a simple chemical method at 200 °C for 2 hours. With increasing pH to 12, the results of XRD showed hematite (α-Fe_2O_3) formation in both cases. The average crystallite sizes were found to be around 16.71nm when PH 1.6 and 21.65 nm when PH 12. SEM image showed a micrograph of the nanoparticle structures observed with the particle size of 40.06 nm. When the pH is increased to 12, different shapes are formed in the same sample. The NPs aggregation of small NPs to Sheet shape and cubic with particle size 61.22 and 45.56 nm respectively. UV–vis measurements showed the energy band increased from 3.11eV to 5.11eV. The antimicrobial activity of iron oxide NPs was determined by growth inhibition zones of the negative gram bacteria *E. coli*, *Klebsiella spp*, and positive gram bacteria *S. aureus*, *S. epidermidis*, and fungal *Candida albicans*. The zones for (α-Fe2O3) NPs are when PH 1.6 was between (12-13) mm. The zones for (α-Fe2O3) NPs are when PH 12 was a little higher between (13-15) mm.

REFERENCES

[1] Fatimah I: Green synthesis of silver nanoparticles using extract of Parkia speciosa Hassk pods assisted by microwave irradiation. *Journal of advanced research* 2016, 7(6):961-969.

[2] Vasantharaj S, Sathiyavimal S, Senthilkumar P, LewisOscar F, Pugazhendhi A: Biosynthesis of iron oxide nanoparticles using leaf extract of Ruellia tuberosa: antimicrobial properties and their applications in photocatalytic degradation. *Journal of Photochemistry and Photobiology B: Biology* 2019, 192:74-82.

[3] Abid MA, Kadhim DA: Novel comparison of iron oxide nanoparticle preparation by mixing iron chloride with henna leaf extract with and without applied pulsed laser ablation for methylene blue degradation. *Journal of Environmental Chemical Engineering* 2020, 8(5):104138.

[4] Nagajyothi P, Pandurangan M, Kim DH, Sreekanth T, Shim J: Green synthesis of iron oxide nanoparticles and their catalytic and in vitro anticancer activities. *Journal of Cluster Science* 2017, 28(1):245-257.

[5] Demirezen DA, Yıldız YŞ, Yılmaz Ş, Yılmaz DD: Green synthesis and characterization of iron oxide nanoparticles using Ficus carica (common fig) dried fruit extract. *Journal of bioscience and bioengineering* 2019, 127(2):241-245.

[6] Mody VV, Siwale R, Singh A, Mody HR: Introduction to metallic nanoparticles. *Journal of Pharmacy and Bioallied Sciences* 2010, 2(4):282.

[7] Bouafia A, Laouini SE: Green synthesis of iron oxide nanoparticles by aqueous leaves extract of Mentha Pulegium L.: Effect of ferric chloride concentration on the type of product. *Materials Letters* 2020, 265:127364.

[8] Lohrasbi S, Kouhbanani MAJ, Beheshtkhoo N, Ghasemi Y, Amani AM, Taghizadeh S: Green Synthesis of Iron Nanoparticles Using Plantago major Leaf Extract and Their Application as a Catalyst for the Decolorization of Azo Dye. *BioNanoScience* 2019, 9(2):317-322.

[9] Chauhan S, Upadhyay LSB: Biosynthesis of iron oxide nanoparticles using plant derivatives of Lawsonia inermis (Henna) and its surface modification for biomedical application. *Nanotechnology for Environmental Engineering* 2019, 4(1):8.

[10] Varadavenkatesan T, Selvaraj R, Vinayagam R: Dye degradation and antibacterial activity of green synthesized silver nanoparticles using Ipomoea digitata Linn. flower extract. *International Journal of Environmental Science and Technology* 2019, 16(5):2395-2404.

[11] Zhang L, Jiang Y, Ding Y, Daskalakis N, Jeuken L, Povey M, O'Neill AJ, York DW: Mechanistic investigation into antibacterial behaviour of suspensions of ZnO nanoparticles against E. coli. *Journal of Nanoparticle Research* 2010, 12(5):1625-1636.